

Highly Emissive and Electrochemically Stable Thienylene Vinylene Oligomers and Copolymers: An Unusual Effect of Alkylsulfanyl Substituents

By Shehzad Jeeva, Olena Lukoyanova, Athan Karas, Afshin Dadvand, Federico Rosei, and Dmitrii F. Perepichka*

The synthesis, unexpected efficient photoluminescence, and reversible electrochemical p- and n-doping of new conjugated thienylene vinylene materials functionalized with alkylsulfanyl substituents poly(trithienylene vinylene) (PTTV) and poly(dithienylvinyl-co-benzothiadiazole) (PDTVB) along with dithienylvinylene-based oligomers is reported. The materials are studied by thermal and X-ray diffraction analysis, optical spectroscopy, cyclic voltammetry, and spectroelectrochemistry. Organic field-effect transistors (OFETs) are fabricated with PTTV and PDTVB. The polymers, prepared by Stille polycondensation, exhibit good thermal stability and a photoluminescent quantum yield in the range 34%–68%. Low bandgaps (1.5–1.8 eV), estimated by optical and electrochemical measurements along with high stability of both redox states, suggest that these structures are promising materials for photovoltaic applications. OFETs fabricated with PDTVB reveal a hole mobility of $7 \times 10^{-3} \text{ cm}^2 \text{ V}^{-1} \text{ s}^{-1}$ with on/off ratio 10^5 , which are comparatively high values for completely amorphous polymer semiconductors.

devices by solution processing of conjugated polymers is particularly appealing for large-area optoelectronic applications.^[2] Significant progress in the field of organic electronics has already led to the commercialization of highly efficient, bright, and multicolored thin-film displays based on a range of organic light-emitting diode (OLED) devices.^[3] At the same time, organic field-effect transistors (OFETs)^[4] and organic photovoltaics (OPVs),^[5] despite major recent advancements, are still facing issues of material performance and stability that need to be addressed before wide commercial applications are realized.

Polythiophenes are generally considered as some of the most promising candidate materials in large area optoelectronics.^[6] In particular, regioregular poly(3-hexylthiophene) (P3HT, Formula 1), which has a bandgap of ~ 1.9 eV, has shown superior semiconducting performance with hole

1. Introduction

Conjugated polymers with aromatic and/or heteroaromatic backbones have attracted wide attention as plastic semiconductors, with a plethora of applications that span across the fields of light-emitting diodes, photovoltaic cells, field-effect transistors, chemical and biosensors, and so on.^[1] Much of the interest is due to the fact that the properties of these materials can be readily tuned on a molecular level to address specific applications. Moreover, the prospect of manufacturing low-cost and/or flexible electronic

mobility up to $0.1 \text{ cm}^2 \text{ V}^{-1} \text{ s}^{-1}$ and is still the benchmark polymeric material for OFETs and OPVs.^[6] Nevertheless, there is still a significant interest in tuning the electronic structure of polythiophenes to further improve their charge carrier mobility, enhance the luminescence quantum yield (which is rather low in most polythiophenes), and reduce the bandgap to be able to capture a large portion of the solar spectrum in OPV applications. One of the major approaches to such tuning is the reduction of the aromatic stabilization (which hampers electron delocalization), for example, by introducing donor-acceptor or aromatic-quinoidal structural disturbances.^[7,8] Diluting the aromaticity by alternating benzene rings with vinylene groups has been a particularly fruitful approach leading to the famous poly(phenylene vinylene) (PPV) and thousands of its derivatives, which were the first and still are some of the most extensively investigated polymers in OLED applications.^[9]

The thiophene analog of PPV, poly(thienylene vinylene) (PTV), however, has attracted relatively limited attention.^[10–16] This is somewhat surprising considering the substantial bandgap reduction in PTV ($1.7 \text{ eV}^{[10,14]}$ compared to $\sim 2 \text{ eV}$ for polythiophene^[6] and 2.5 eV for PPV^[9c]), the relatively high hole mobility measured in OFETs based on PTV^[17] and its copolymers,^[18,19] and the high conductivity in the doped state.^[20] One of the major drawbacks of PTV materials is the dramatic loss of emissive properties (quantum yield $\Phi_{\text{PL}} \sim 0.001\%$ for parent PTV^[21]). The lack of

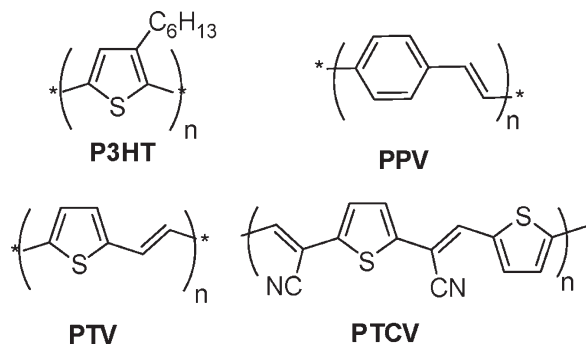
[*] Prof. D. F. Perepichka, Dr. S. Jeeva, Dr. A. Karas, Dr. O. Lukoyanova, A. Dadvand

Department of Chemistry McGill University
Montreal, Quebec, H3A 2K6 (Canada)
E-mail: dmitrii.perepichka@mcgill.ca

Prof. F. Rosei, A. Dadvand
Centre Énergie, Matériaux et Télécommunications Institut
National de la Recherche Scientifique Varennes
Quebec J3X 1S2 (Canada)

Prof. D. F. Perepichka, Prof. F. Rosei
Centre for Self-Assembled Chemical Structures McGill
University Montreal, Quebec, H3A 2K6 (Canada)

DOI: 10.1002/adfm.200902300



Formula 1. Structures of discussed conjugated polymers.

photoluminescence (PL) in PTV and its derivatives has been noted by several authors and is well-accepted in the literature.^[21–25] Although PL was reported for a few PTV copolymers with large fluorophoric groups (fluorene,^[26,27] biquinoline,^[28] and carbazole^[29]) their efficiency was relatively low; all PTV homopolymers and copolymers with small fluorophoric groups (e.g., benzothiadiazole,^[30] thiophene-*S,S*-dioxide^[24a]) are not emissive. To the contrary, PTV acts as an efficient luminescence quencher.^[13] A large number of thienylene vinylene oligomers have also been studied,^[31] yet no efficient emitters have been reported so far.

The reason for this loss of emissive properties is not clear. Early studies^[21] attributed the lack of PL to the effect of sulfur and enhanced conjugation (which leads to fast exciton–exciton recombination). While this is plausible, it does not explain why the PL of PTV is much lower than that of polythiophene. A very low singlet-to-triplet gap in PTV oligomers, which could lead to fast intersystem crossing and quench the singlet excited state, was predicted by time-dependent density functional theory calculations (TD-DFT).^[32] Also, the low efficiency of PL of the smallest building block of PTV, dithienylvinylene (DTV) (which is still higher than that of PTV: 1% in nonpolar solvents, 5% in butyronitrile) was attributed to a symmetry-forbidden transition from the lowest excited state.^[33] It is also likely that synthesis-related impurities and/or backbone defects provide an additional quenching pathway for some PTV polymers. Indeed, the majority of synthetic approaches to PTV and its derivatives were based on either a thermal conversion route (heating a soluble precursor >200 °C)^[10,13–15,21] or oxidative^[11,15] polymerization. While the thermal conversion route does not appear to be a problem for PPV materials, one could expect thiophene rings to be less stable in these conditions. An important exception is due to alkyl-substituted poly(thiophene cyanovinylene) (PTCV), which was synthesized by more gentle Knoevenagel condensation and showed near-IR (NIR; 950 nm) emission.^[34,35] Most recently the NIR PL (724 nm) was found in alkoxy-carbonyl-substituted PTV, although the PL quantum yield was not reported for either of these polymers.^[36]

Revisiting PTV materials as possible precursors for ladder-type thienoacene,^[37,38] we have synthesized several alkylsulfanyl-substituted thienylvinylene oligomers and surprisingly found these to be highly luminescent materials. We thus decided to investigate whether highly emissive properties can be generally engineered in electron-rich PTV materials and if such properties can be combined with a low bandgap and high charge mobility, which are typical for

many thiophene-based polymers. Here, we describe the synthesis and characterization of poly(trithienylene vinylene) (PTTV), its donor–acceptor analog poly(dithienylvinylene-*co*-benzothiadiazole) (PDTVB), and three model oligomers. We report tunable (deep-blue to deep-red) and efficient PL, reversible electrochemical p- and n-doping with corresponding in situ spectroscopic characterization, as well as the OFET performance of the synthesized materials.

2. Results and Discussion

2.1. Synthesis

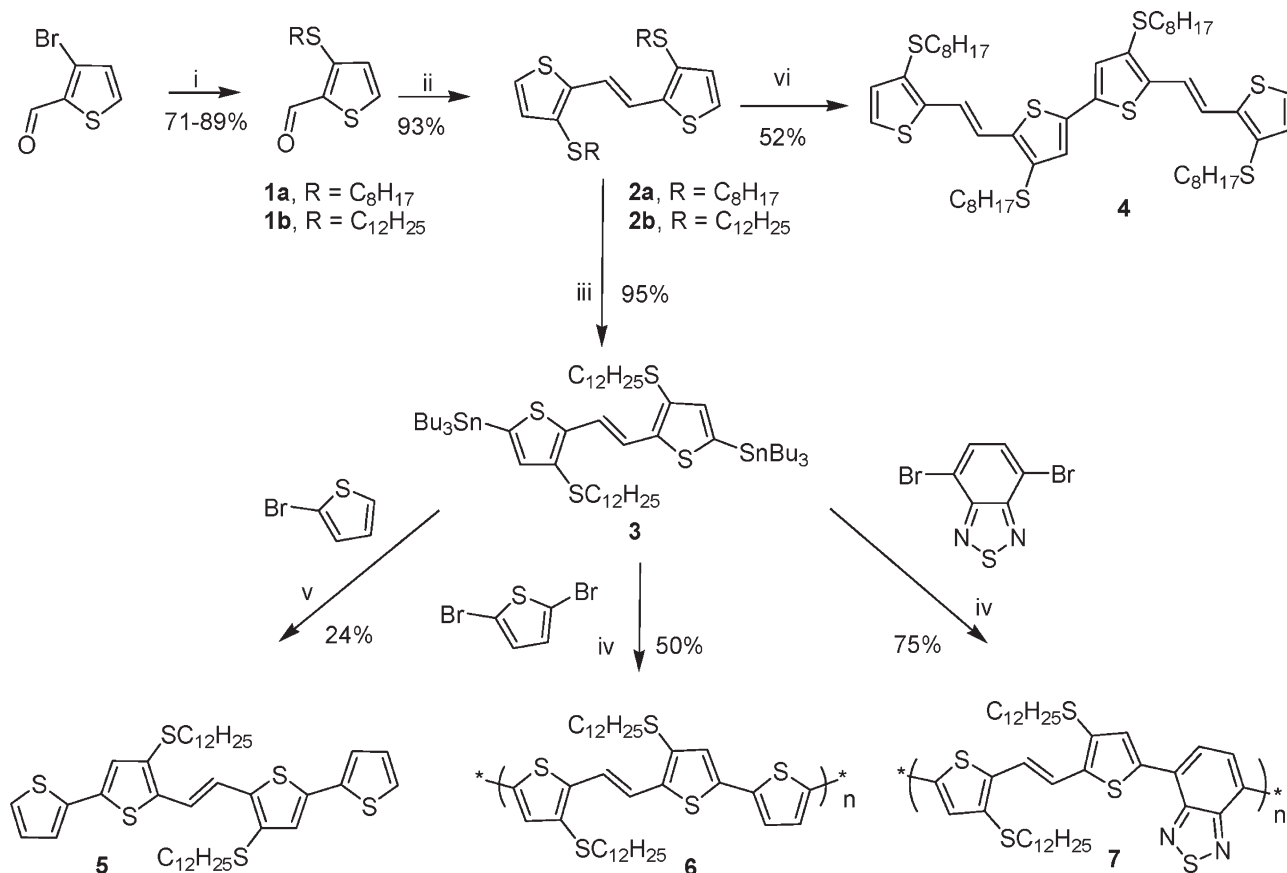
The synthesis of the key monomer (**2**, Scheme 1) involved the conjugate addition-elimination of alkylthiol to 3-bromothiophene-2-carbaldehyde to afford corresponding sulfide **1**, followed by McMurry coupling to give pure *E*-1,2-bis(3-(dodecylthio)thien-2-yl)vinylene **2**. Attempts to synthesize dibromo- and diiodo-derivatives of **2** under various conditions failed, probably due to the presence of an active vinylene unit. In fact, the intramolecular cyclization of related 3-alkylthio-2-vinylthiophenes derivatives by action of I₂ was previously reported.^[37] Successful functionalization of **2** was, however, achieved by stannylation of the dilithium derivative of **2** with tributyltin chloride (to give intermediate **3**) as well as oxidative dimerization of its monolithium salt with CuCl₂ (to give oligomer **4**).

The synthesis of PTTV **6** and PDTVB **7** was accomplished by Stille polycondensation using equimolar amounts of 2,5-dibromothiophene or 4,7-dibromobenzothiadiazole, respectively, and monomer **3**. The dark purple polymers were purified by reprecipitation from dichloromethane (DCM) with methanol followed by Soxhlet extraction of short oligomers with hexane. The molecular weight (MW) and the polydispersity index (PDI) were assessed by gel-permeation chromatography (GPC) and matrix-assisted laser-desorption ionization time-of-flight (MALDI-TOF) analyses, which showed a moderate MW of 24 700 g mol⁻¹ with PDI of 1.45 for **6** and MW of 8000 g mol⁻¹ with PDI of 2.0 for **7**. These relatively low MWs are typical for Stille coupling polymerization and the wide distribution of polymer chain lengths might be partially responsible for the amorphous nature of **6** and **7**. Another model oligomer **5** was synthesized using similar Stille coupling with 2-bromothiophene.

Thermogravimetric analysis (TGA) of the dithienyleneethene monomer **2b** and polymers **6** and **7** (in N₂ atmosphere) reveals a reasonably high thermal stability with decomposition onsets >300 °C. Differential scanning calorimetry (DSC) shows no phase transitions for both polymers in the temperature range –10–250 °C. Also, X-ray diffraction (XRD) analysis shows no sign of crystallinity in either of the polymers (see Supporting Information).

2.2. Optical Properties

The optical properties of new materials **2** and **4–7** were measured in tetrahydrofuran (THF) solutions and in thin films (for **6** and **7**). The DTV **2** is a pale-yellow solid with absorption maxima in the UV region of the spectrum (364 nm). Extending the conjugation through endcapping with thiophene rings (**5**) or through



Scheme 1. i) RSH, K₂CO₃, DMF, rt, 12 h; ii) TiCl₄, Zn, THF, reflux, 2 h; iii) n-BuLi (2.5 M in hexanes), tributyltinchloride, THF, -78 °C to rt; iv) Pd(PPh₃)₄, DMF, 130 °C, N₂, 24 h; v) Pd(PPh₃)₄, toluene, reflux, N₂, 24 h; vi) n-BuLi (2.5 M in hexanes), CuCl₂, THF.

dimerization (**4**) leads to a predictable red shift (60–100 nm) of the absorption (Table 1, Fig. 1). The much larger bathochromic shift experienced by polymer **6** (>200 nm) suggests a rather long effective conjugation length. The red-edge of the absorption band gives the optical band gap of 1.83 eV for **6**. It can be further reduced by employing a well-known donor–acceptor alternation strategy.^[7] Indeed, incorporating an electron-poor benzothiadiazole unit in **7** lowers the band gap to 1.65 eV. In the solid state the bandgap absorption of both polymers undergoes a red shift of ~50–100 nm as a result of intermolecular π - π interactions (Fig. 2). The effect is somewhat stronger for benzothiadiazole-containing **7**, which

shows a very low optical bandgap of 1.48 eV in condensed phase (compared to 1.75 eV for **6**). No further bandgap decrease was observed upon annealing the polymer film by exposing to CHCl₃ vapors^[39] or by heating at 120 °C for 48 h, in agreement with the amorphous nature of the materials (see Supporting Information). We note that the low bandgap and the very broad absorption of **7** that covers the entire visible spectrum make it of great potential interest for photovoltaic applications.

Rather unexpectedly, all DTV derivatives, including **6** and **7**, showed bright PL (Table 1, Fig. 1). The emission color changes as the bandgap is decreased with extending the conjugation and

Table 1. Optical characteristics of compounds **2b** and **4–7**.

Compound	THF solution				Thin films		
	$\lambda_{\max}^{\text{abs.}}$ [nm]	$\lambda_{\max}^{\text{PL}}$ [nm]	Φ_{PL} (%)	$E_{\text{g}}^{\text{opt}}$ [eV]	$\lambda_{\max}^{\text{abs.}}$ [nm]	$\lambda_{\max}^{\text{PL}}$ [nm]	$E_{\text{g}}^{\text{opt}}$ [eV]
2b	364	426	32[d]	2.95	–	–	–
4	467	572	21[c]	2.25	–	–	–
5	428	523	49[c]	2.48	–	–	–
6	574	655	68[a]	1.83	588	680	1.75
7	586	702	34[b]	1.65	670	700	1.48

[a] Zinc phthalocyanine in 1% pyridine/toluene solution as a reference ($\lambda_{\max}^{\text{PL}}$ range 660–750 nm, $\Phi_{\text{PL}} = 0.30$).^[47] [b] Nile Blue in methanol as a reference ($\Phi_{\text{PL}} = 0.27$).^[47] [c] Fluorescein in 0.1 M aq. NaOH as a reference ($\Phi_{\text{PL}} = 0.79$).^[1] [d] Anthracene in ethanol as a reference ($\Phi_{\text{PL}} = 0.27$).^[47]

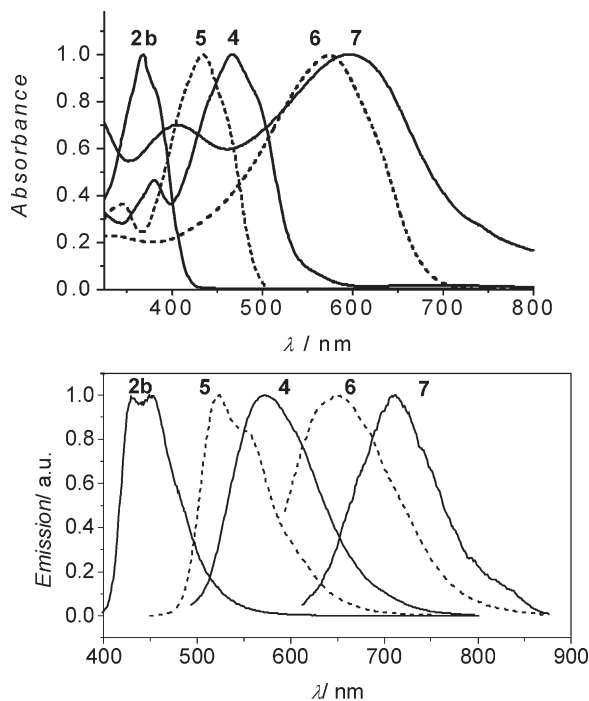


Figure 1. UV-Vis absorption (top) and PL (bottom) spectra of thienylene vinylene derivatives **2** and **4–7** in THF solution.

covers the full range from deep-blue ($\lambda_{\text{max}}^{\text{PL}}$ 426 nm for **2b**) to deep-red ($\lambda_{\text{max}}^{\text{PL}}$ 702 nm for **7**). The PL efficiency, Φ_{PL} , of up to 68% (for **6**, Table 1) is not only much higher than that of all previously reported thienylene vinylene polymers (most of which are not emissive) but also higher than that of all thiophene homopolymers ($\Phi_{\text{PL}} \leq 25\%$).^[22]

We attribute this enhanced fluorescence to the effect of the alkylsulfanyl group on the thiophene ring. Indeed, the analogs of these materials with alkyl,^[13,40] alkoxy,^[23] phenyl,^[14] or no substituents^[21] are not emissive. Such enhancement is rather surprising since introducing sulfur atoms in a fluorophore usually leads to enhanced intersystem crossing and dramatically suppresses the PL quantum yield. In order to understand the effect of the alkylsulfanyl group, we performed DFT calculation of the **2** and its derivatives with methylsulfanyl (**2'**) and ethyl (**2''**) substituents at the B3LYP/6-31G(d) level. The results clearly show that alkylsulfanyl group acts as a moderate electron-acceptor,

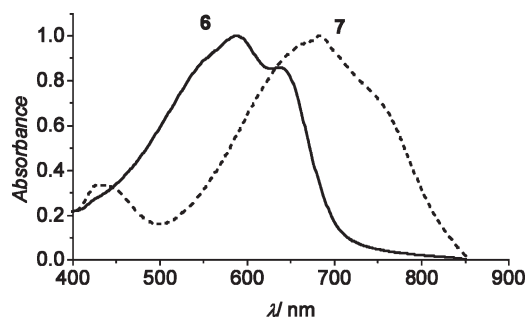


Figure 2. UV-Vis absorption of **6** and **7** in thin films.

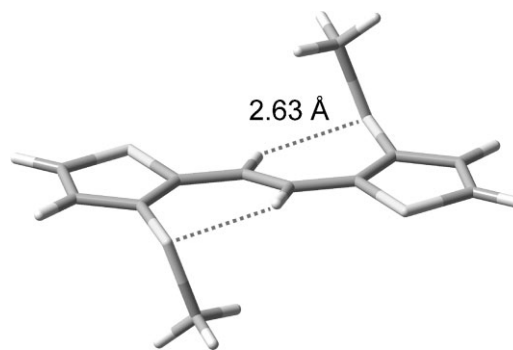


Figure 3. DFT-optimized structure of model oligomer **2'** showing a preferred out-of-plane orientation of alkylsulfanyl substituent enforced by hydrogen bonding with vinyl protons.

reducing the HOMO energy from -5.20 eV in **2** (-5.19 eV in **2''**) to -5.37 eV for **2'**. We note that the HOMO energy of **2'** is in excellent agreement with the value obtained for its longer alkyl chain analog **2b** by electrochemistry (see below). A lowered HOMO reduces the risk of oxidation (doping) by oxygen, which is a common problem in electron-rich polythiophenes and could certainly contribute to the quenching of the PL in majority of PTV derivatives. In fact, the only emissive PTVs reported are those containing electron-withdrawing groups: cyano-substituted PTCV^[34,35] and recently reported alkoxy-carbonyl-substituted PTV.^[36]

The minimal energy conformation of **2'** (Fig. 3) shows a slight twist (8°) between the thiophene ring and the vinylene moiety, which should not significantly affect the conjugation. The methylsulfanyl substituents are out-of-plane, which allows the sulfur atoms to engage its lone pair in a hydrogen-bonding interaction with vinylene protons (S...H distance is 2.63 Å). This conformation is preferred versus the fully planar structure by 1.2 kcal mol⁻¹. The out-of-plane orientation of the alkyl chains should result in “screening” of the conjugated polymer backbone by substituents preventing close $\pi \cdots \pi$ interaction and further reducing the risk of PL quenching through excimer formation.

2.3. Electrochemistry

The electrochemical properties of oligomers **2b**, **4**, and **5** were investigated by cyclic voltammetry (CV, Fig. 4) and the obtained redox potentials were used to determine the HOMO/LUMO energies (Table 2). The shortest oligomer **2b** shows an irreversible oxidation wave with current peak potential of $E_{\text{pa}} = 0.57$ V versus Fc/Fc⁺, indicating a chemical instability of a radical cation on an isolated thiophene ring. The following partially reversible redox waves at 0.88 and 1.25 V versus Fc/Fc⁺ must be due to the product(s) of the first oxidation. However, no polymer film formation was observed on the electrode surface upon multiple potential cycling (for concentrations up to 20 mM). No reduction process was detected by CV within the potential window, consistent with the large optical bandgap of **2b**. The bithiophene moiety in the structure of **5** stabilizes the ion radical species and two reversible one-electron oxidation waves as well as a partially reversible reduction wave were observed in its CV.

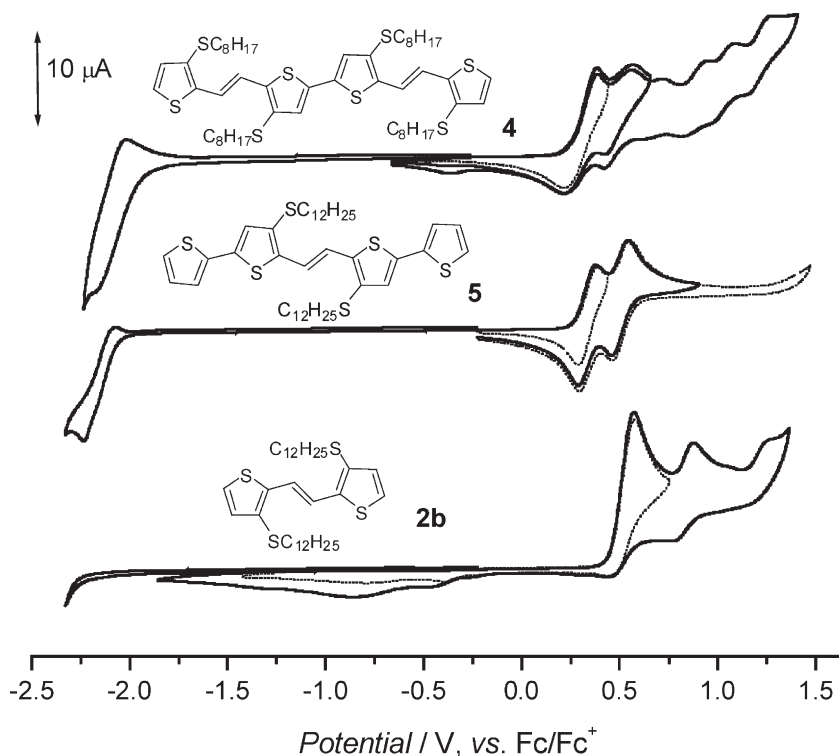


Figure 4. CVs of 1.1 mm oligo(thienylene vinylene)s in 0.1 M TBAPF₆/CH₂Cl₂; scan rate: 0.1 V s⁻¹.

The first oxidation peak of **5** is 250 mV less positive than that of DTV **2**, indicating a raised HOMO level due to the extended conjugation. A very similar effect was observed for the DTV dimer **4**. However, while the first oxidation giving **4**^{•+} was (quasi)reversible, removing the second electron (presumably from the terminal monothiophene moieties) is irreversible. The second oxidation is followed by four consecutive oxidation waves (twice the number observed for corresponding “monomer” **2b** at 0.72, 0.95, 1.07, and 1.25 V versus Fc/Fc⁺). These redox waves were not observed for the shorter oligomer **5**, highlighting the reactivity of the monothiophene-centered radical-cation in these structures. Similar oligomers, without alkyldithiophenyl groups, were reported to undergo only two reversible electrochemical oxidations under similar conditions.^[41] This fact, along with the lack of concentration dependence and of film growth on the electrode suggest that

intramolecular reaction, rather than electro-oxidative polymerization, contributes to the electrochemical irreversibility.

Both **6** and **7** show a further reduction of the HOMO–LUMO gap from the oligomers **4** and **5**. Both polymers also exhibit reversible p- and n-doping behavior, as seen from their CVs in Figure 5. The bandgaps, 1.98 eV for **6** and 1.67 eV for **7**, were determined from differential pulse voltammetry (DPV, see Supporting Information). These values were somewhat higher, yet in reasonable agreement with the optical bandgaps (Table 1). Replacing the thiophene moiety with electron-deficient benzothiadiazole in **7** significantly facilitates the n-doping, while the p-doping is only slightly disfavored as compared to **6**. The electrochemical bandgap of **7** is also consistent with the bandgaps reported for polymers with the same backbone structures, but different substitution pattern (alkoxy groups).^[30] Interestingly, the alkylsulfanyl substituents seem to significantly increase the electrochemical n-doping stability of **7**. Two discernible reduction processes were observed for **7** in propylene carbonate and acetonitrile (see Supporting Information) since it was sufficiently stable at more negative potentials. Multiple potential cycling (100 cycles in propylene carbonate) of the first reduction process, within the –1.8 to –0.1 V versus Fc/Fc⁺

potential range, resulted in less than 9% loss of cathodic peak current intensity (see Supporting Information). The second reduction is slightly less reversible and an additional 60 cycles, including first and second reduction processes (i.e., up to –2.2 V vs. Fc/Fc⁺), resulted in a ~40% loss of electrochemical signal.

Spectroelectrochemical experiments further confirmed excellent stability of both polymers toward p-doping, even without any protection from the atmospheric oxygen and moisture. Polymer **6** exhibits distinct color switching from purple to black upon electrochemical oxidation. The absorption spectrum of the neutral polymer film began to change at 0.6 V (vs. Ag wire), consistent with the onset p-doping potential under these experimental conditions. The bandgap absorption band at $\lambda_{\text{max}} = 650$ nm decreases while two new broad polaronic absorption bands (at $\lambda_{\text{max}} \sim 1000$ nm and >1600 nm) start to grow (Fig. 6, solid lines). An isosbestic point at

Table 2. Redox potentials[a] and HOMO–LUMO levels of **2b**, **4**, and **5** in solution and **6** and **7** in thin films.

Compnd	$E_{\text{red}}^{\text{PC}}/E_{\text{red}}^{\text{PA}}$	$E_{\text{red}}^{1/2}$	$E_{\text{ox1}}^{\text{PA}}/E_{\text{ox1}}^{\text{PC}}$	$E_{\text{lox}}^{1/2}$	HOMO[b]	LUMO[b]	$E_{\text{gap}}[\text{b}]$
2b	–	–	0.57/–	–	–5.37	–	>2.9
4	–2.02/–2.16	2.09	0.38/0.22	0.30	–5.1	–2.71	2.36
5	–2.08/–2.40	2.24	0.38/0.29	0.34	–5.14	–2.56	2.58
6	–	–1.91[c]	–	0.16[d]	–4.96	–2.89	1.98
7	–	–1.55[c]	–	0.26[d]	–5.06	–3.25	1.67

[a] All potentials are reported in volts versus Fc/Fc⁺ redox couple. [b] HOMO and LUMO energies and bandgaps are determined from CV for solution (0.1 M TBAPF₆/CH₂Cl₂) and DPV for films (0.1 M TBAPF₆/propylene carbonate as an electrolyte) according to $E_{\text{MO}} = -4.8 - E_{\text{red/ox}}$ versus Fc/Fc⁺ and reported in eV. [c] $E_{\text{red}}^{\text{onset}}$. [d] $E_{\text{ox}}^{\text{onset}}$.

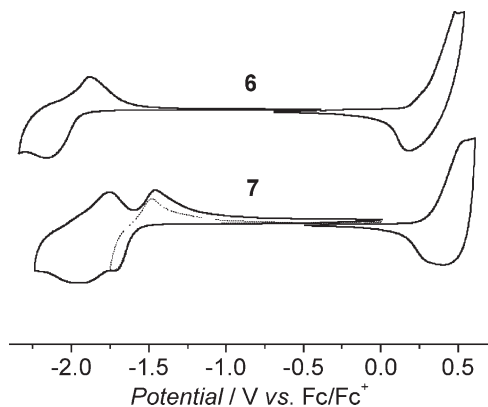


Figure 5. CVs of **6** and **7** films in 0.1 M TBAPF₆/propylene carbonate; scan rate: 0.1 V s⁻¹.

~750 nm is maintained during these spectral changes, up to +0.95 V potential, suggesting a clean transition between the neutral and polaronic state. Different spectral characteristics (a band at ~800 nm and a very broad absorption >1100 nm) start to develop above +0.95 V, which is consistent with formation of bipolaronic states (Fig. 6, dashed lines). Upon reduction back to 0 V, the absorption spectrum resumed its original (undoped) shape.

Very similar spectroelectrochemical behavior was observed for **7** (see Supporting Information), although due to limited spectral changes in the visible region (400–700 nm), the polymer retained its dark-blue appearance throughout electrochemical oxidation in the 0 to 1.3 V (vs. Ag wire) range with spectral recovery upon re-reduction to the neutral form.

2.4. FET Studies

Thin-film transistors were prepared in bottom-contact configuration by spin-coating a chlorobenzene solution of **6** and **7** on Si/SiO₂ substrates prepatterned with Au electrodes. The transistor output and transfer characteristics are shown in Figure 7. OFETs based on **6** showed low hole mobilities (up to $4 \times 10^{-5} \text{ cm}^2 \text{ V}^{-1} \text{ s}^{-1}$). However, much higher hole mobilities (up to $7 \times 10^{-3} \text{ cm}^2 \text{ V}^{-1} \text{ s}^{-1}$) were found for thiadiazole-containing **7**. The amorphous natures

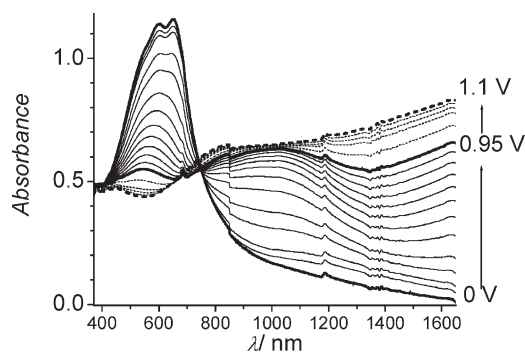


Figure 6. Spectroelectrochemistry of **6** film in 0.1 M TBAPF₆/propylene carbonate; potential is versus Ag wire pseudo-reference electrode, spectra collected in 25 mV intervals.

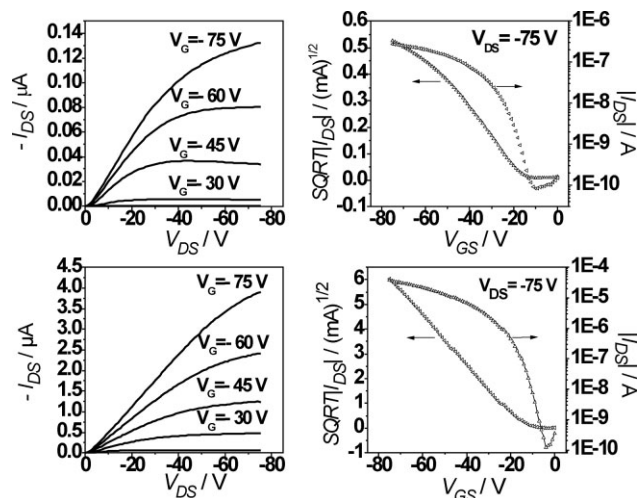


Figure 7. Output (left) and transfer (right) characteristics of OFET based on **6** (top, $\mu_h = 4 \times 10^{-5} \text{ cm}^2 \text{ V}^{-1} \text{ s}^{-1}$; on/off ratio 10^3) and **7** (bottom, $V_T = -10 \text{ V}$; $\mu_h = 7 \times 10^{-3} \text{ cm}^2 \text{ V}^{-1} \text{ s}^{-1}$; on/off ratio 10^5 ; $V_T = -25 \text{ V}$).

of **6** and **7**, while having the advantage of simplified device manufacturing (no need of annealing and uniform performance unaffected by the degree of crystallinity), clearly limits the charge mobility in these materials. No signs of crystallization (based either on XRD or optical absorption data) was observed during annealing of the polymer films by heating at temperatures up to 120 °C or by exposure to chloroform vapor. Accordingly, these treatments did not improve device performance. While mobilities approaching $10^{-2} \text{ cm}^2 \text{ V}^{-1} \text{ s}^{-1}$ are far from the champion values for organic semiconductors in crystalline form, they are quite close to the best mobilities observed in amorphous organic semiconductors.^[19,42] We also note that the on/off ratio of 10^5 achieved by **7** is quite high as for solution-processed device.

3. Conclusions

In summary, we have demonstrated the synthesis and characterization of highly emissive, low-bandgap conjugated polymers **6** and **7**, along with corresponding model oligomers **2**, **4**, and **5**. We found that the alkylsulfanyl group, aside from a predictable improvement of solubility, causes unexpected electronic effects dramatically increasing the emissivity of these thienylene vinylene derivatives and improving their electrochemical stability. Indeed, while most of thienylene vinylene derivatives show no or marginal fluorescence, a PL quantum yield of 68% and 34% was measured for **6** and **7**, respectively. DFT calculations reveal the electron-withdrawing effect of the alkylsulfanyl group and the preferred out-of-plane orientation of the alkyl chain that could minimize the quenching of the PL by oxygen-doped states and formation of excimers, respectively. Further synthetic exploration of the alkylsulfanyl substituents in conjugated materials thus seems justified.^[43]

Excellent stability of both p- and n-doped states of the synthesized polymers was demonstrated by repeated CV as well as spectroelectrochemical studies. The bandgap energies (~1.7 eV

for **6**, ~ 1.5 eV for **7**) make these polymers potential candidates for OPV. The OFET device fabricated with **7** showed an un-optimized hole mobility of up to $7 \times 10^{-3} \text{ cm}^2 \text{ V}^{-1} \text{ s}^{-1}$, which is a reasonably high value for completely amorphous solution-processed materials. Further work is under progress to fabricate a photovoltaic device from **7**.

4. Experimental

Materials and Methods: All reactions were carried out under dry nitrogen atmosphere. The reagents *n*-butyllithium (1.6 and 2.5 M in hexanes), tributyltin chloride, palladium (II) chloride (Alfa Aesar), triphenylphosphine, *N*-bromosuccinimide, and thiophene were obtained commercially (from Aldrich, except where noted) and used without further purification. IR spectra were obtained on a Nicolet 6700 FTIR spectrometer in an ATR mode. ^1H NMR and ^{13}C NMR spectra were obtained on a Varian Mercury 300 or 400 MHz NMR spectrometer. Mass spectra were run on a Kratos 7525 RFA (EI, 70 eV) or ThermoFisher Orbitrap (ESI and APCI) mass spectrometer. UV-Vis spectra were measured with a Varian Cary 5000 spectrometer in 1 cm cuvettes or in films spin-coated on microscope glass slide. GPC analysis was performed on a Viskotek (TDA model 301) instrument using polystyrene standards, conventional calibration (1.0 mL min^{-1} in THF). Fluorescence spectra were measured with a Varian Eclipse spectrofluorometer in 1 cm cuvettes (in solution) or in films spin-coated on microscope glass slide. Φ_{PL} of **2b** and **4–7** was measured in THF solution related to appropriate standards (Table 1) as described before [44].

Electrochemical Measurements: All electrochemical measurements were performed at room temperature in a three-electrode cell using a CHI-770 Electrochemical Workstation. Electrochemical investigations of oligomers **2b**, **4**, and **5** were conducted in anhydrous CH_2Cl_2 with a Pt disk ($d = 1.6 \text{ mm}$) as the working electrode, Pt wire as the auxiliary electrode, and Ag/Ag^+ as the non-aqueous reference electrode. Solutions of **6** and **7** in chloroform were drop-cast on a Pt disk and electrochemical measurements were performed in propylene carbonate with Pt wire and Ag/AgCl electrodes. All potentials were referenced against Fc/Fc^+ redox couple, which in our conditions show 0.38 V versus Ag/Ag^+ in CH_2Cl_2 and 0.41 V versus Ag/AgCl in propylene carbonate. Bu_4NPF_6 (0.1 M) was used as a supporting electrolyte. The electrolyte solution was purged with Ar gas before and between electrochemical measurements.

Spectroelectrochemistry: For spectroelectrochemical measurements, solutions of **6** and **7** in chloroform were drop-cast on freshly cleaned (sonication in acetone, then O_2 -plasma) indium tin oxide (ITO)-coated glass and the substrate was dried in vacuum. This polymer-coated working electrode was immersed in a 1-cm quartz cuvette containing 0.1 M $\text{Bu}_4\text{NPF}_6/\text{PC}$, and Pt gauze and Ag wire were placed in the same cuvette as the counter and pseudo-reference electrodes, respectively. Prior to spectral characterization, the polymer films were electrochemically cycled within 0 to 1 V until a reproducible electrochemical response was obtained. The progressive doping potentials were then set to the ITO electrode and after the doping was complete (evaluated by dropping of the current, ca. 3 min) the spectral absorption was recorded.

OFET Device Fabrication and Testing: OFETs were fabricated using single-channel Au source/drain electrodes (bottom-contact configuration) patterned on 190-nm-thick SiO_2 thermally grown on heavily *n*-doped Si ($\rho \sim 0.01\text{--}0.02 \text{ Ohm cm}$). The thickness of the electrodes was 25 nm. Au patterning was achieved by lift off using a 5-nm-thick Cr adhesion layer [45]. Prior to deposition, substrates were cleaned by sonication in acetone and isopropyl alcohol followed by plasma cleaning. Then, Si/ SiO_2 surfaces were modified with hexamethyldisilazane (HMDS). The substrates were placed in HMDS/toluene (10%) solution and held at 90°C for 1 h, then washed with acetone to remove excess of HMDS and dried under a N_2 gas stream. The single-channel devices had channel length of $6 \mu\text{m}$ and widths of $1880 \mu\text{m}$. The semiconductor films were deposited from a concentrated solution of both compounds by spin-coating with velocity ranging from 500 to 1200 rpm.

The charge-carrier mobilities of OFETs were calculated in the saturation regime on the reverse scan, from a plot of the square root of the drain current versus gate voltage using

$$I_{\text{DS}} = C_i \mu (W/2L)(V_G - V_T)^2 \quad (1)$$

where I_{DS} is the drain-source current, C_i the capacitance per unit area of the gate dielectric (18 nF cm^{-2}), L the channel length, W the channel width, and V_T and V_G are the threshold voltage and gate voltage, respectively. Electrical measurements were carried out at room temperature under vacuum (10^{-6} mbar) using a LakeShore probe station and Keithley 4200 semiconductor parameter analyzer.

3-Bromothiophene-2-carbaldehyde [47]: To a solution of diisopropylamine (25.0 mL, 184 mmol) in anhydrous THF (300 mL) in a three-neck 1 L round bottom flask equipped with a thermometer, magnetic stirrer bar, and septum seal, was added *n*-BuLi (73.5 mL, 2.5 M in hexane, 184 mmol) and the mixture was stirred at $\sim 0\text{--}8^\circ\text{C}$ for 20 min. To the prepared solution of lithium diisopropylamide (LDA), 3-bromothiophene (30.0 g, 184 mmol, 17.3 mL) was added dropwise via syringe keeping the temperature $< 5^\circ\text{C}$. The resultant mixture was stirred for 30 min with continuous cooling in ice water, followed by dropwise addition of *N*-methylformanilide (22.7 mL, 184 mmol) over ca. 20 min. Following a period of 3 h with stirring, 1.0 M HCl (200 mL) was added and the heterogeneous mixture was stirred for 30 min. Et_2O (100 mL) was added and the organic phase was separated and washed with 1.0 M HCl (200 mL) and brine (200 mL) and dried over anhydrous MgSO_4 . After filtration through a plug of silica and evaporation in vacuo, the crude material was dried under high vacuum, giving the yellow oil of the desired product (31.3 g, 89%), which was of sufficient purity for further reaction. ^1H NMR (300 MHz, CDCl_3 , δ): 9.98 (s, 1H; CHO), 7.72 (d, $J = 5.1 \text{ Hz}$, 1H; Ar-H), 7.16 (d, $J = 5.4 \text{ Hz}$, 1H; Ar-H); IR: $\nu = 1649 \text{ cm}^{-1}$.

4,7-Dibromobenzothiadiazole: This was prepared according to the published procedure [46] by bromination of benzothiadiazol, which results in a white solid (1.1 g, 50% yield), m.p. $187\text{--}188^\circ\text{C}$ [46]. The monomer was used without further characterization.

3-Dodecylsulfanylthiophene-2-carbaldehyde (1b): K_2CO_3 (27.0 g, 195 mmol), 3-bromothiophene-2-carbaldehyde [47] (15.0 g, 78.1 mmol), and dodecane-1-thiol (19.0 g, 22.5 mL, 93.7 mmol) were added to DMF (250 mL). The resultant amber brown mixture was stirred at room temperature for 2 days during which time it changes to brick brown colored. The mixture was poured into brine (400 mL) and extracted with EtOAc (500 mL). The organic phase was separated and dried over MgSO_4 . Evaporating the solvent gives a pale yellow oil (30.7 g) that was purified via column chromatography (1:20 EtOAc/Hex) followed by recrystallization in EtOH to give **1b** as yellow crystals (17.0 g, 71%), m.p. $24\text{--}25^\circ\text{C}$. ^1H NMR (300 MHz, CDCl_3 , δ): 10.08 (s, 1H; CHO), 7.71 (d, $J = 4.8 \text{ Hz}$, 1H; Ar-H), 7.19 (d, $J = 5.4 \text{ Hz}$, 1H; Ar-H), 2.98 (t, $J = 7.6 \text{ Hz}$, 2H; SCH_2), 1.65 (m; CH_2), 2.4–1.2 (m; CH_2), 0.87 (t, $J = 6.8 \text{ Hz}$, 3H; CH_3); ^{13}C NMR (75 MHz, CDCl_3 , δ): 182.1 (C=O), 145.0, 138.5, 134.4, 129.4, 34.6, 31.9, 29.6, 29.5, 29.4, 29.3, 29.1, 28.6, 22.6, 14.1; IR: $\nu = 1649 \text{ cm}^{-1}$; HRMS (EI, m/z): $[\text{M}^+]$ calcd for $\text{C}_{12}\text{H}_{28}\text{OS}_2$, 312.15816; found, 312.15719.

3-Octylsulfanylthiophene-2-carbaldehyde (1a): This was prepared exactly as **1b** using octanethiol. The product was obtained as a yellow oil (2.98 g, 89%). ^1H NMR (300 MHz, CDCl_3 , δ): 10.08 (s, 1H; CHO), 7.71 (d, $J = 5.2 \text{ Hz}$, 1H; Ar-H), 7.11 (d, $J = 5.2 \text{ Hz}$, 1H; Ar-H), 2.99 (t, $J = 7.6 \text{ Hz}$, 2H; SCH_2), 1.66 (m, 2H; CH_2), 1.44 (m, 2H; CH_2), 1.26 (m, 8H; CH_2), 0.87 (t, $J = 6.8 \text{ Hz}$, 3H; CH_3); IR: $\nu = 1649 \text{ cm}^{-1}$.

E-1,2-Bis(3-(dodecylsulfanylthienyl)-2)ethene (2b): To an ice-cold stirred suspension of Zn dust (0.68 g) in anhydrous THF (100 mL) was added TiCl_4 (3.6 g, 2 mL) dropwise. The resultant mixture was refluxed for 90 min, during which time dissolution of yellow-green precipitate was attained to afford a black solution. On cooling at 45°C the aldehyde **1b** (2.0 g, 6.4 mmol) dissolved in THF (15 mL) was added in one portion via septum seal and the reaction mixture was stirred overnight at room temperature. A saturated solution of NaHCO_3 (200 mL) and CHCl_3 (60 mL) was added and the mixture was stirred for 2 h after which it was filtered, separated into organic and aqueous phases, and the aqueous phase extracted with CHCl_3

(30 mL). The combined organic phases were dried over MgSO_4 , filtered, and evaporated in vacuo to give a crude brownish-yellow oil, which was purified by column chromatography (EtOAc /petroleum ether 1:30) to afford the yellow product **2b** (1.77 g, 93% yield), m.p. 64–66 °C (from CHCl_3 -methanol). $^1\text{H NMR}$ (300 MHz, CDCl_3 , δ): 7.36 (s, 2H; =CH), 7.17 (d, 2H, $J = 5.2$ Hz; Ar-H), 7.01 (d, $J = 5.6$ Hz, 2H; Ar-H), 2.78 (t, $J = 7.0$ Hz, 4H; SCH_2), 1.56 (m, 4H; CH_2), 1.24 (m, 36H; CH_2), 0.87 (t, $J = 6.6$ Hz, 6H; CH_3); $^{13}\text{C NMR}$ (75 MHz, CDCl_3 , δ): 141.9, 132.0, 130.7, 123.5, 120.9, 36.5, 32.0, 29.7, 29.6, 29.5, 29.3, 29.3, 28.7, 22.8, 14.2; IR: $\nu = 1462$ cm^{-1} ; HRMS (EI, m/z): $[\text{M}^+]$ calcd for $\text{C}_{34}\text{H}_{56}\text{S}_4$, 592.3265; found, 592.3259; TGA: $T_{\text{dec}} = 293$ °C (onset).

E-1,2-Bis(3-octylsulfanylthien-2-yl)ethene (2a): Prepared exactly as **2b** as yellow powder (730 mg, 52% yield); m.p. 46–48 °C (from CHCl_3 -methanol). $^1\text{H NMR}$ (300 MHz, CDCl_3 , δ): 7.37 (s, 2H; =CH), 7.17 (d, 2H, $J = 4.8$ Hz; Ar-H), 7.01 (d, $J = 5.2$ Hz, 2H; Ar-H), 2.79 (t, $J = 7.5$, 4H; SCH_2), 1.56 (m, 4H; CH_2), 1.40 (m, 4H; CH_2), 1.24 (m, 16H; CH_2), 0.87 (t, $J = 6.9$ Hz, 6H; CH_3); $^{13}\text{C NMR}$ (75 MHz, CDCl_3 , δ): 142.1, 132.2, 130.9, 123.6, 121.0, 36.7, 32.0, 29.9, 29.44, 29.38, 28.8, 22.9, 14.3; TGA: $T_{\text{dec}} = 300$ °C (onset).

E-1,2-Bis(3-dodecylsulfanyl-5-(tributylstannyl)thienyl-2)ethene (3): To a solution of **2b** (200 mg, 0.33 mmol) in anhydrous THF (80 mL) was added *n*-BuLi (0.34 mL, 0.84 mmol, 2.5 M in Hex) dropwise at -78 °C and stirred at room temperature for 2 h. The reaction mixture was again cooled to -78 °C and to the above intermediate, tributyltin chloride (0.2 mL, 0.74 mmol) was added via syringe and the reaction mixture was stirred for 36 h at room temperature. A saturated solution of Na_2CO_3 (150 mL) was added, followed by the addition of EtOAc (100 mL). The organic layer was dried (MgSO_4), filtered, and evaporated under vacuum to give yellowish brown oil. The yellow oil was passed through a plug of silica column (hexane) to give tin derivative **3** (361 mg, 95%), which was used without further purification. $^1\text{H NMR}$ (300 MHz, CDCl_3 , δ): 7.35 (s, 2H), 7.01 (s, 2H), 2.78 (t, $J = 6.8$ Hz, 4H; SCH_2), 1.61–1.07 (m, 76H; CH_2), 0.87 (m, 24H; CH_3); IR: $\nu = 1463$ cm^{-1} ; MS (APCI) 1171.53 $[\text{M}-\text{H}^+]$.

4,4'-Bis(octylsulfanyl)-5,5'-bis[2-(3-octylsulfanylthien-2-yl)vinyl-1]-[2,2']bithiophene (4): **2a** (1.00 g, 2.07 mmol) was charged into a flame-dried three-neck round-bottomed flask equipped with a thermometer. Under an argon atmosphere, Et_2O (20 mL) was added and the resultant green/yellow solution was cooled to -78 °C. To the above suspension, *n*-BuLi (2.5 M in hexane; 0.9 mL, 2.25 mmol) was added dropwise and warmed to 0 °C for 3 h. CuCl_2 was added under positive pressure and a red color formed instantly. The resultant reaction mixture was left stirring at room temperature overnight. The resultant blood-red mixture was diluted with Et_2O (20 mL) and washed with deionized water (20×3 mL) and brine (20 mL). The organic layer was separated and dried over anhydrous MgSO_4 , filtered, and evaporated in vacuo to afford a viscous red oil. Purification by column chromatography (hexane/ EtOAc ; 20:1) gave red solid product (520 mg, 52%), m.p. 56–58 °C. $^1\text{H NMR}$ (400 MHz; CDCl_3 , δ): 7.34 (s, 4H), 7.18 (d, $J = 5.2$, 2H), 7.10 (s, 2H), 7.02 (d, $J = 5.2$ Hz, 2H), 2.83 (m, 8H), 1.60 (m, 8H), 1.42 (m, 8H), 1.26 (m, 32H), 0.86 (m, 12H); ^{13}C (75 MHz; CDCl_3 , δ): 141.5, 137.0, 134.4, 132.18, 132.15, 128.5, 124.0, 121.2, 120.5, 36.71, 36.68, 32.1, 29.790, 29.85, 29.5, 29.4, 28.88, 28.85, 22.9, 14.4; IR: $\nu = 1466$ cm^{-1} ; UV/Vis (THF): $\lambda_{\text{max}}(\epsilon) = 467$ nm; PL (THF): $\lambda_{\text{max}}(\epsilon) = 572$ nm; HRMS (APCI, m/z): $[\text{M}+\text{H}^+]$ calcd for $\text{C}_{52}\text{H}_{79}\text{S}_8$, 959.3942; found, 959.3927.

E-1,2-Bis(3-(dodecylsulfanyl)-5-(thien-2-yl)thien-2-yl)ethene (5): To an oven dried round-bottomed flask, 2-bromothiophene (0.17 mg, 1.06 mmol), **3** (250 mg, 0.48 mmol), and $\text{Pd}(\text{PPh}_3)_4$ (4 mol %) were added and dissolved in toluene (10 mL). The system was degassed and then heated to 60 °C under argon atmosphere overnight. The reaction mixture was cooled to room temperature. The organic layer was washed with deionized water (50×3 mL) and brine (50 mL). The organic layer was separated and dried over anhydrous MgSO_4 , filtered, and evaporated in vacuo to afford a crude red solid that was purified by recrystallization from DCM/ EtOH mixture to give red needles of **5b** (86 mg, 24%), m.p. 84–86 °C. $^1\text{H NMR}$ (300 MHz, CDCl_3 , δ): 7.31 (s, 2H), 7.28 (s, 2H), 7.22 (d, $J = 5.2$ Hz, 2H), 7.09 (s, 2H), 7.02 (d, $J = 5.2$ Hz, 2H), 2.83 (t, $J = 6.8$ Hz, 4H; $-\text{SCH}_2$), 1.60 (m, 4H; $-\text{CH}_2$), 1.41–1.24 (m, 36H; $-\text{CH}_2$), 0.86 (t, $J = 6.6$ Hz, 6H; $-\text{CH}_3$); IR: $\nu = 1468$ cm^{-1} ; HRMS (APCI, m/z): $[\text{M}+\text{H}^+]$ calcd for $\text{C}_{42}\text{H}_{61}\text{S}_6$ $[\text{MH}^+]$, 757.3092; found, 757.3081.

PTTV 6: To a mixture of monomer **3** (597 mg, 0.51 mmol) and 2,5-dibromothiophene (122 mg, 0.51 mmol) in thoroughly degassed DMF (10 mL) was added $\text{Pd}(\text{Ph}_3\text{P})_4$ (10 mol%) and the mixture was stirred at 90 °C under N_2 for 48 h. The reaction mixture was cooled to room temperature and then passed through a plug of silica and evaporated in vacuo. The dark purple residue was purified by repeated precipitation ($\times 3$) from CHCl_3 solution with MeOH, then by extraction with hexane and dried under vacuum to give **6** (50%). $^1\text{H NMR}$ (400 MHz, CDCl_3 , δ): 7.19–6.89 (broad), 2.84 (broad, s), 1.67–1.23 (broad, m), 0.86 (broad, m); IR: $\nu = 1452$ cm^{-1} ; TGA: $T_{\text{dec}} = 347.3$ °C (onset); UV/Vis (THF): $\lambda_{\text{red-edge}} = 667$ nm; GPC (THF): MW = 24 700 g mol^{-1} . PDI = 1.45; MALDI-TOF: 42 000 (maximum intensity). Further purification can be achieved by prolonged (12 h) Soxhlet extraction with hexane. The hexane insoluble fraction of **6** (25%) shows a slightly shifted absorbance ($\lambda_{\text{red-edge}} = 680$ nm) but no improvement in hole mobility measured in OFET devices. GPC (THF): MW = 30 700 g mol^{-1} . PDI = 1.33.

PDTV 7: To a mixture of monomer **3** (501 mg, 0.42 mmol) and 4,7-dibromobenzothiadiazole (125 mg, 0.42 mmol) in thoroughly degassed DMF (10 mL) was added $\text{Pd}(\text{Ph}_3\text{P})_4$ (10 mol %) and the mixture was stirred at 90 °C under the atmosphere of N_2 for 48 h. The reaction mixture was cooled to room temperature and passed through a plug of silica and evaporated. The dark purple residue was purified by repeated precipitation process using CHCl_3 as solvent to solubilize and cold MeOH to precipitate. After the repeated precipitation process ($\times 3$) from CHCl_3 solution with MeOH and the further purification by Soxhlet using hexane the dark purple precipitate was dried under high vacuum to give **7** (75%). $^1\text{H NMR}$ (400 MHz, CDCl_3 , δ): 8.2–8.0 (broad) 7.85–7.0 (broad)–6.89 (broad), 2.91 (broad, m), 1.9–0.6 (broad, m); IR: $\nu = 1482$ cm^{-1} ; TGA: $T_{\text{dec}} = 346.7$ °C (onset); UV/Vis (THF): $\lambda_{\text{red-edge}} = 750$ nm; GPC (THF): MW = 8000 g mol^{-1} , PDI = 2.0.

Acknowledgements

We acknowledge support from NSERC of Canada through Discovery Grants and a CRD grant supported by Plasmionique Inc. We are grateful to the CFI for infrastructure support. F.R. acknowledges the Canada Research Chairs program for partial salary support. We thank Nadim Saade (McGill University) and Dr. Patrick Pribil (MDS Analytical Technologies) for mass-spectrometry analyses and Petr Fiuhrasek (CSACS, McGill University) for GPC. Supporting Information includes detailed electrochemical and spectroelectrochemical analyses, XRD and MALDI-TOF data for the polymers, and details of DFT calculations. Supporting Information is available online from Wiley InterScience or from the authors.

Received: December 7, 2009

Revised: January 22, 2010

Published online: April 7, 2010

- [1] *Handbook of Conducting Polymers*, 3rd Ed. (Eds: T. A. Skotheim, J. R. Reynolds) CRC Press, New York 2007.
- [2] S. R. Forrest, *Nature* 2004, 428, 911.
- [3] Z. R. Li, H. Meng, *Organic Light-emitting Materials and Devices*, CRC Press, Boca Raton, FL 2006.
- [4] S. Allard, M. Forster, B. Souharce, H. Thiem, U. Scherf, *Angew. Chem.* 2008, 120, 4138; *Angew. Chem, Int. Ed.* 2008, 47, 4070.
- [5] a) S. E. Shaheen, D. S. Ginley, G. E. Jabbour, *MRS Bull.* 2005, 30, 10. b) Y. J. Cheng, S.-H. Yang, C.-S. Hsu, *Chem. Rev.* 2009, 109, 5868. c) E. Bundgaard, F. C. Krebs, *Solar Ener. Mater. Solar Cells* 2007, 9, 954.
- [6] *Handbook of Thiophene-Based Materials*, Vol. 2 (Eds: I. F. Perepichka, D. F. Perepichka) John Wiley & Sons, New York 2009.
- [7] J. Roncali, *Chem. Rev.* 1997, 97, 173.
- [8] M. D. Zaman, D. F. Perepichka, *Chem. Commun.* 2005, 4187.

- [9] a) J. H. Burroughes, D. D. C. Bradley, A. R. Brown, R. N. Marks, R. H. Friend, P. L. Burn, A. B. Holmes, *Nature* **1990**, *347*, 593. b) A. C. Grimsdale, K. L. Chan, R. E. Martin, P. G. Jokisz, A. B. Holmes, *Chem. Rev.* **2009**, *109*, 897. c) D. F. Perepichka, I. F. Perepichka, H. Meng, F. Wudl, in *Organic Light-emitting Materials and Devices* (Eds: Z. R. Li, H. Meng) CRC Press, Boca Raton, FL **2006**.
- [10] a) S. Yamada, S. Tokito, T. Tsutsui, S. Saito, *J. Chem. Soc., Chem. Commun.* **1987**, 1148. b) H. Murata, S. Tokito, T. Tsutsui, S. Saito, *Synth. Met.* **1990**, *36*, 95.
- [11] R. Galarini, A. Musco, R. Pontellini, A. Bolognesi, S. Destri, M. Catellani, M. Mascherpa, G. Zhuo, *J. Chem. Soc., Chem. Commun.* **1991**, 364.
- [12] M. Catellani, S. Luzzati, A. Musco, F. Speroni, *Synth. Met.* **1994**, *62*, 223.
- [13] W. J. Mitchell, C. Pena, P. L. Burn, *J. Mater. Chem.* **2002**, *12*, 200.
- [14] A. Henckens, K. Colladet, S. Fourier, T. J. Cleij, L. Lusten, J. Gelan, D. Vanderzande, *Macromolecules* **2005**, *38*, 19.
- [15] Y. Fu, H. Cheng, R. L. Elsenbaumer, *Chem. Mater.* **1997**, *9*, 1720.
- [16] M. Henckens, M. Knipper, I. Polec, J. Manca, L. Lusten, D. Vanderzande, *Thin Solid Films* **2004**, *451*, 572.
- [17] H. Fuchigami, A. Ysumura, H. Koezuka, *Appl. Phys. Lett.* **1993**, *63*, 1372.
- [18] B. Lim, K.-J. Baeg, H.-G. Jeong, J. Jo, H. Kim, J.-W. Park, Y.-Y. Noh, D. Vak, J.-H. Park, J.-W. Park, D.-Y. Kim, *Adv. Mater.* **2009**, *21*, 2808.
- [19] D. S. Chung, S. J. Lee, J. W. Park, D. B. Choi, D. H. Lee, J. W. Park, S. C. Shin, Y.-H. Kim, S.-K. Kwon, C. E. Park, *Chem. Mater.* **2008**, *20*, 3450.
- [20] T. Benincori, E. Brenna, F. Sannicolò, L. Trimarco, G. Schiavon, S. Zecchin, G. Zotti, *Macromol. Chem. Phys.* **1996**, *197*, 517.
- [21] A. J. Brassett, N. F. Colerani, D. D. C. Bradley, R. A. Lawrence, R. H. Friend, H. Murata, S. Tokito, T. Tsutsui, S. Saito, *Phys. Rev. B* **1990**, *41*, 10586.
- [22] I. F. Perepichka, D. F. Perepichka, H. Meng, F. Wudl, *Adv. Mater.* **2005**, *17*, 2281.
- [23] J. Mei, N. C. Heston, S. V. Vasilyeva, J. R. Reynolds, *Macromolecules* **2009**, *42*, 1482.
- [24] C. Zhang, T. H. Nguyen, J. Sun, R. Li, S. Black, C. E. Bonner, S.-S. Sun, *Macromolecules* **2009**, *42*, 663.
- [25] J. Hou, Z. Tan, Y. He, C. Yang, Y. Li, *Macromolecules* **2006**, *39*, 4657.
- [26] U. Asawapirom, R. Güntner, M. Forster, T. Farrel, U. Scherf, *Synthesis* **2002**, *9*, 1136.
- [27] B. Chen, Y. Wu, M. Wang, S. Wang, S. Sheng, W. Zhu, R. Sun, H. Tian, *Eur. Polym. J.* **2004**, *40*, 1183.
- [28] C. J. Tonzola, M. M. Alam, S. A. Jenekhe, *Macromolecules* **2005**, *38*, 9539.
- [29] J.-F. Morin, N. Drolet, Y. Tao, M. Leclerc, *Chem. Mater.* **2004**, *16*, 4619.
- [30] P. M. Beaujuge, S. V. Vasilyeva, S. Ellinger, T. D. McCarley, J. R. Reynolds, *Macromolecules* **2009**, *42*, 3694.
- [31] a) J. Roncali, *Acc. Chem. Res.* **2000**, *33*, 147. b) P. Blanchard, P. Verlhac, P.; L. Michaux, P. Frere, J. Roncali, *Chem. Eur. J.* **2006**, *12*, 1244.
- [32] F. C. Grozema, P. T. Van Duijnen, L. D. A. Siebbeles, A. Goossens, S. W. De Leeuw, *J. Phys. Chem. B* **2004**, *108*, 16139.
- [33] G. Bartocci, A. Spalletti, R. S. Becker, F. Elisei, S. Floridi, U. Mazzucato, *J. Am. Chem. Soc.* **1999**, *121*, 1065.
- [34] P. Wagner, P.-E. Aubert, L. Lutsen, D. Vanderzande, D., *Electrochem. Commun.* **2002**, *4*, 912.
- [35] S. C. Moratti, R. Servini, A. B. Holmes, D. R. Baigent, R. H. Friend, N. C. Greenham, J. Grüner, P. J. Hamer, *Synth. Metals* **1995**, *71*, 2117.
- [36] L. Huo, T. L. Chen, Y. Zhou, J. Hou, H.-U. Chen, Y. Yang, Y. Li, *Macromolecules* **2009**, *42*, 4377.
- [37] a) T. Yamamoto, K. Takiyama, *J. Am. Chem. Soc.* **2007**, *129*, 2224. b) T. Yamamoto, E. Miyazaki, K. Takiyama, *Heterocycles* **2008**, *78*, 583.
- [38] K. Oyaizu, T. Iwasaki, Y. Tsukahara, E. Tsuchida, *Macromolecules* **2004**, *37*, 1257.
- [39] M. R. Andersson, D. Selse, M. Berggren, H. Järvinen, T. Hjertberg, O. Inganäs, O. Wennerstrom, J.-E. Osterholm, *Macromolecules* **1994**, *27*, 6503.
- [40] J. J. Apperloo, C. Martineau, P. A. van Hal, J. Roncali, R. A. J. Janssen, *J. Phys. Chem. A* **2002**, *106*, 21.
- [41] P. Frère, J.-M. Raimundo, P. Blanchard, J. Delaunay, P. Richomme, J.-L. Sauvajol, J. Orduna, J. Garin, J. Roncali, *J. Org. Chem.* **2003**, *68*, 7254.
- [42] J. Veres, S. D. Ogier, S. W. Leeming, D. C. Cupertino, S. M. Khaffaf, *Adv. Funct. Mater.* **2003**, *13*, 199.
- [43] H. J. Spencer, P. J. Skabara, M. Giles, I. McCulloch, S. J. Coles, M. B. Hursthouse, *J. Mater. Chem.* **2005**, *15*, 4783.
- [44] L. Porres, A. Holland, L.-O. Pålson, A. P. Monkman, C. Kemp, A. Beeby, *J. Fluoresc.* **2006**, *16*, 267.
- [45] C. Santato, F. Cicoira, P. Cosseddu, A. Bonfiglio, P. Bellutti, R. Zamboni, M. Muccini, F. Rosei, A. Mantoux, P. Doppelt, *Appl. Phys. Lett.* **2006**, *88*, 163511.
- [46] B. A. Da Silveira Neto, A. Sant'Ana Lopes, G. Ebeling, R. S. Gonçalves, V. E. U. Costa, F. H. Quina, J. Dupont, *Tetrahedron* **2005**, *61*, 10975.
- [47] L. S. Fuller, B. Iddon, K. A. Smith, *J. Chem. Soc. Perkin Trans. 1* **1997**, 3465.